LIN-41 inactivation leads to delayed centrosome elimination and abnormal chromosome behavior during female meiosis in *Caenorhabditis elegans*

Rieko Matsuura[a], Tomoko Ashikawa[a], Yuka Nozaki[a], and Daiju Kitagawa[a,b,*]

[a]Division of Centrosome Biology, Department of Molecular Genetics, National Institute of Genetics, Mishima, Shizuoka 411-8540, Japan; [b]Department of Genetics, School of Life Science, SOKENDAI, Mishima, Shizuoka 411-8540, Japan

ABSTRACT During oogenesis, two successive meiotic cell divisions occur without functional centrosomes because of the inactivation and subsequent elimination of maternal centrosomes during the diplotene stage of meiosis I. Despite being a conserved phenomenon in most metazoans, the means by which this centrosome behavior is controlled during female meiosis remain elusive. Here, we conducted a targeted RNAi screening in the *Caenorhabditis elegans* gonad to identify novel regulators of centrosome behavior during oogenesis. We screened 513 genes known to be essential for embryo production and directly visualized GFP–γ-tubulin to monitor centrosome behavior at all stages of oogenesis. In the screening, we found that RNAi-mediated inactivation of 33 genes delayed the elimination of GFP–γ-tubulin at centrosomes during oogenesis, whereas inactivation of nine genes accelerated the process. Depletion of the TRIM-NHL protein LIN-41 led to a significant delay in centrosome elimination and to the separation and reactivation of centrosomes during oogenesis. Upon LIN-41 depletion, meiotic chromosomes were abnormally condensed and pulled toward one of the two spindle poles around late pachytene even though the spindle microtubules emanated from both centrosomes. Overall, our work provides new insights into the regulation of centrosome behavior to ensure critical meiotic events and the generation of intact oocytes.

INTRODUCTION

The centrosome comprises a pair of centrioles surrounded by pericentriolar material (PCM) and serves as the major microtubule-organizing center (MTOC) in most animal cells (Nigg and Stearns, 2011; Bornens, 2012; Bornens *et al.*, 2014; Gönczy, 2012). MTOC activity of centrosomes is crucial for proper chromosome segregation in mitosis and in meiosis during spermatogenesis. By contrast, during oogenesis in most metazoans, maternal centrosomes are inactivated because of the gradual loss of PCM components and are thereafter eliminated during meiotic prophase I; hence, two successive meiotic cell divisions occur without centrosomes (Sathananthan *et al.*, 1996; Delattre and Gönczy, 2004; Manandhar *et al.*, 2005; Schatten and Sun, 2009). The elimination of maternal centrosomes and the inheritance of paternal centrosomes to the progeny are crucial for maintaining the precise number of centrosomes in the fertilized zygote and thus for proper sexual reproduction.

The gonad of the *Caenorhabditis elegans* hermaphrodite is a well-suited model for analyzing the mechanisms governing centrosome behavior during oogenesis because all stages of oogenesis can be seen in a continuous manner within a single gonad (Hubbard and Greenstein, 2000). To reduce successfully the number of centrosomes in oocytes, as the first step, centrosomes lose the ability to nucleate microtubules around the transition zone (TZ) during meiosis (Kemp *et al.*, 2004; Mikeladze-Dvali *et al.*, 2012). As the second step, elimination of centrioles occurs in the loop region of the gonad during the diplotene stage (Mikeladze-Dvali *et al.*, 2012). The

Abbreviations used: CCT, chaperonin-containing TCP-1; CDK, cyclin-dependent kinase; GCN, germ cell nuclei; GFP, green fluorescent protein; MTOC, microtubule-organizing center; NEBD, nuclear envelope breakdown; pCDK-1, phospho-CDK-1; PCM, pericentriolar material; RNAi, RNA interference; TZ, transition zone.

developing oocytes from which centrioles were previously eliminated arrest in meiotic prophase I until the resumption of meiotic maturation by the major sperm protein (MSP; Kim et al., 2013). During late prophase of meiosis I, the synaptonemal complex, a protein complex that mediates the pairing of homologous chromosomes during meiosis, disassembles before meiotic spindle formation begins (Zetka et al., 1999; Hansen et al., 2004). The cyclin-dependent kinase 1 (CDK-1)/cyclin B complex, a maturation-promoting factor (MPF), is required for both mitotic and meiotic spindle formation with or without centrosomes (McCarter et al., 1999; Burrows et al., 2006; Kim et al., 2010). Therefore, to prevent ectopic activation of centrosomes, CDK-1/cyclin B activity must be suppressed until centrosome elimination is completed in oocytes.

Although the molecular mechanisms responsible for the inactivation and elimination of centrosomes during oogenesis remain elusive, the RNA helicase CGH-1 has been reported to promote timely centriole elimination in C. elegans germ cells (Mikeladze-Dvali et al., 2012). Cosuppression of the CDK inhibitor CKI-2 has been shown to perturb centrosome elimination in the same model system (Dae and Roy, 2006). However, in germ cells of cki-2-null mutant hermaphrodites, centrosome elimination is rarely affected (Buck et al., 2009; Mikeladze-Dvali et al., 2012). Because little is known about how centrosomes are inactivated and eliminated in a timely manner during oogenesis, we sought to identify such regulators of centrosome behavior using a combination of a semicomprehensive feeding RNA interference (RNAi) screening and direct visualization of centrosomes at all stages of C. elegans oogenesis.

LIN-41 is known to act in the heterochronic pathway that regulates the differentiation and development of somatic cells from larva to adult in C. elegans (Reinhart et al., 2000; Slack et al., 2000). A recent study claimed that LIN-41 prevents the precocious transition to embryonic differentiation and teratoma formation in developing oocytes (Tocchini et al., 2014). Another group demonstrated that LIN-41 regulates meiotic transition from prophase to M phase through the CDK-1 pathway in the female germ cells of C. elegans (Spike et al., 2014a). Although both studies showed the existence of centrosomes in the proximal gonad of lin-41 mutants, it is most likely that the lin-41–mutant oocytes entered M phase directly after the pachytene stage but did not pass through the diplotene stage of meiotic prophase I, during which centrosome elimination normally occurs. Therefore it is not fully understood whether LIN-41 functions in centrosome elimination during the diplotene stage. In our RNAi-based screening, we used mild inactivation of lin-41 to observe the effect of LIN-41 depletion on centrosome elimination in the diplotene and diakinesis stages and identified LIN-41 as a promoter of centrosome elimination during oogenesis. This regulation seems to be independent of the CDK-1 pathway. We also show that ectopic activation of centrosomes led to abnormal behavior of meiotic chromosomes during oogenesis upon LIN-41 depletion.

RESULTS

Identification of genes that participate in the regulation of centrosome behavior during oogenesis

To identify the genes that regulate the precise time of centrosome elimination during oogenesis, we performed RNAi screening in C. elegans gonads that expressed green fluorescent protein (GFP)–γ-tubulin as a centrosome marker. In this system, centrosome behavior during oogenesis can be readily monitored because all stages of female germline development proceed in a continuous manner within a single gonad. To judge the adequate time needed for centrosome elimination, we focused on the three proximal oocytes, −1 to −3 positions away from the spermatheca, which lack centro-

somes in the wild type (Mikeladze-Dvali et al., 2012). Although genome-wide RNAi screening was performed using C. elegans early embryos (Gönczy et al., 2000; Sönnichsen et al., 2005), those screens did not identify any genes whose reduction leads to retention of maternal centrosomes in the embryos. It could be that pleiotropic defects in meiosis hindered such a phenotype in the early embryos. Alternatively, we hypothesized that if maternal centrosomes remain competent to nucleate microtubules during oogenesis, the processes for proper oogenesis and embryo production could be affected. On the basis of these considerations, we selected a set of 513 genes that are essential for proper embryo production in C. elegans (Green et al., 2011) and used RNAi feeding to test the effects of the inactivation of each gene on centrosome behavior during oogenesis.

In the first screening of each gene, we observed gonads of at least 10 adult worms that were treated with RNAi feeding for 24 h. We examined the time of disappearance of GFP–γ-tubulin foci as an indicator of centrosome elimination, which normally occurs around the diplotene stage in meiotic prophase I (Mikeladze-Dvali et al., 2012). We classified the phenotypes into two main categories depending on whether the disappearance of GFP–γ-tubulin foci in the female germline was delayed or accelerated. In wild-type gonads, the GFP–γ-tubulin signal representing centrosomes could be detected from the distal to the loop region of the gonad (Figure 1A). In the screening, the inactivation of 33 genes caused a significant delay in the disappearance of GFP–γ-tubulin foci (Figure 1B and Supplemental Table S1). These included genes related to a variety of biological processes, such as translation, mitotic–meiotic transition, and membrane trafficking. In particular, inactivation of 29 translation-related genes delayed centrosome elimination, which was accompanied by an obvious developmental delay.

To find specific regulators of centrosome elimination, we focused on the other candidate genes (four genes in the table of Figure 1B). GFP–γ-tubulin foci were consistently retained in proximal oocytes depleted of defect in germline development-1 (GLD-1), abnormal cell lineage-41 (LIN-41), ADP-ribosylation factor-1.2 (ARF-1.2), or N-myristoyl transferase-1 (NMT-1; Figures 1B and 2A). Of interest, in oocytes depleted of ARF-1.2 or NMT-1, numerous GFP–γ-tubulin foci were observed in the cytoplasm and, in particular, were found to accumulate around the nucleus in proximal oocytes (Figures 1B and 2A; 14 of 31 and 18 of 30 gonads, respectively). By contrast, earlier elimination of GFP–γ-tubulin foci at centrosomes was detected in the case of RNAi targeting against nine genes (Figure 1B). Eight genes encode γ-tubulin or one of the subunits of the chaperonin-containing TCP-1 (CCT) complex, which act together as a chaperone for tubulin family proteins (Lundin et al., 2008; Saegusa et al., 2014). In gonads depleted of C23G10.8, whose function is not known, most GFP–γ-tubulin foci were weakly stained even in the distal gonad and were not detectable in the TZ by fluorescence microscopy (Figure 2A and Supplemental Table S1; 10 of 10 animals).

In the second assay, we performed immunostaining of the gonads using antibodies against RME-2 (Grant and Hirsh, 1999), a marker of oocyte maturation, to exclude that the defects in centrosome elimination stem from the secondary effects of developmental delay. In the wild type, RME-2 was detected in the cytoplasm from the diplotene stage to the proximal diakinetic oocytes and accumulated particularly at the plasma membrane of the proximal oocytes (Supplemental Figure S1). Centrosomal GFP–γ-tubulin foci were never observed in control mature oocytes that were well stained with RME-2 antibodies (Supplemental Figure S1; 28 gonads). In gld-1(RNAi) animals, although centrosomal GFP–γ-tubulin foci remained in the proximal oocytes, these oocytes were small, round, and
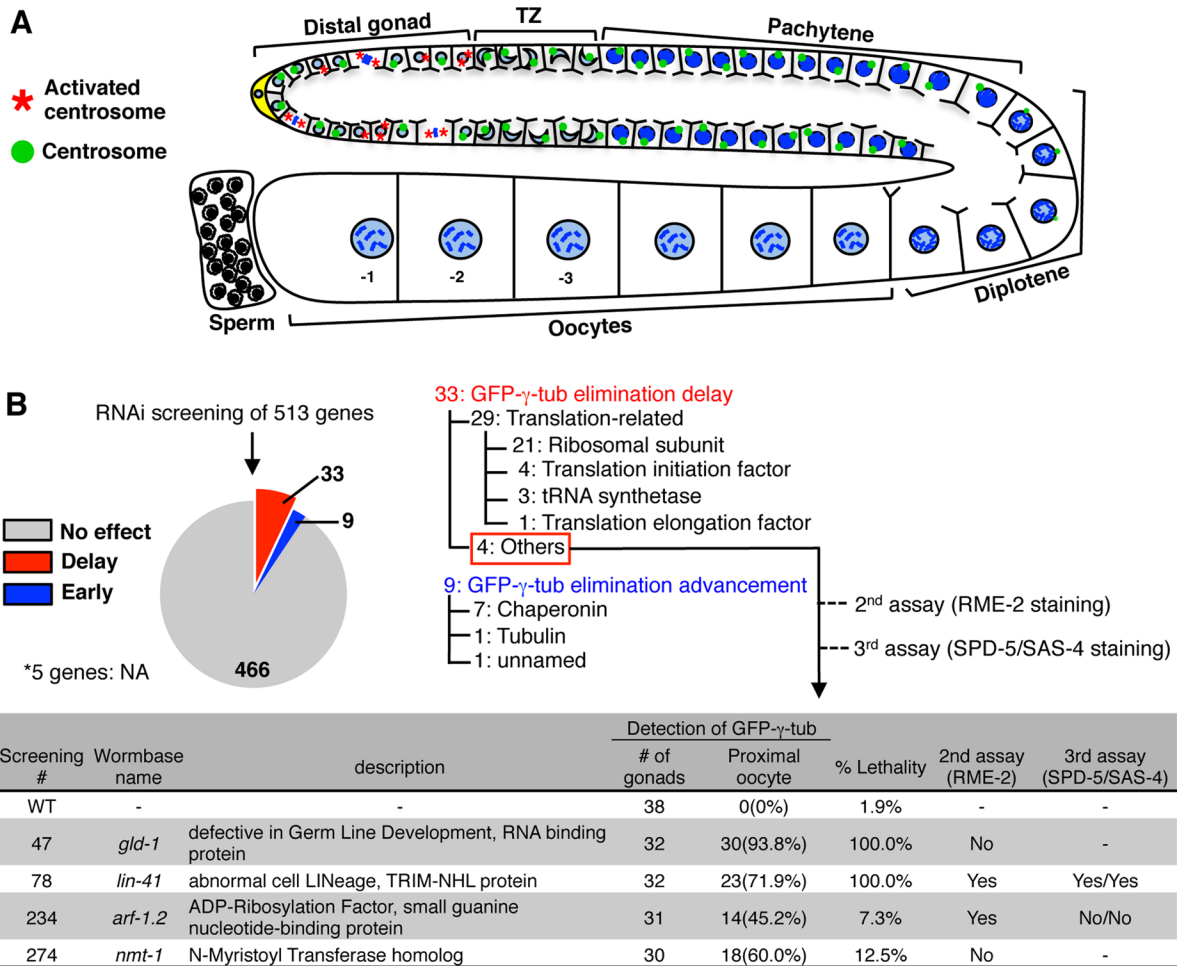
FIGURE 1: Screen to identify genes that participate in the regulation of centrosome behavior during *C. elegans* oogenesis. (A) Schematic of a *C. elegans* hermaphrodite gonad and the time of centrosome inactivation and elimination. Activated centrosomes are observed in mitotic cells in the distal gonad. Centrosome inactivation seems to occur at the transition zone (TZ). Centrosomes are then eliminated during the diplotene stage of meiotic prophase I. Numbers show the position of oocytes from the spermatheca. (B) Screening procedures to narrow down candidate genes regulating centrosome behavior during oogenesis. A total of 513 genes essential for embryo production were inactivated by RNAi feeding for 24 h. Five genes out of 513 genes were not available. Inactivation of 33 and nine genes, respectively, showed GFP–γ-tubulin elimination delay or advance. They were classified according to their biological functions. The phenotype and lethality provoked by inactivation of four genes, listed in the table, were further confirmed in terms of reproducibility. The existence of GFP–γ-tubulin foci in proximal oocytes (−1 to −3 positions away from the spermatheca) was examined. They were subsequently assessed in the second assay (RME-2 staining for testing oocyte maturation) and third assay (SPD-5 and SAS-4 staining for testing PCM and centriole integrity).

RME-2–negative immature oocytes (RME-2 positive; 0 of 13 gonads). In the case of *gld-1(RNAi)*, this is consistent with the fact that female germ cells of the *gld-1* loss-of-function mutant reenter mitosis around the pachytene stage and escape from meiotic prophase (Francis *et al.*, 1995). In *nmt-1(RNAi)* animals, the proximal oocytes seemed to be morphologically fully grown but lacked membrane RME-2 (RME-2 positive; one of 16 gonads). These results suggest that inactivation of *gld-1* and *nmt-1* indirectly caused centrosome elimination delay as a consequence of defective specification of female germ cells or delayed oocyte development. Of importance, coexistence of membrane RME-2 and GFP–γ-tubulin foci was frequently observed in the *arf-1.2(RNAi)* and *lin-41(RNAi)* proximal oocytes (Supplemental Figure S1; RME-2 positive; 18 of 31 gonads in *arf-1.2(RNAi)* and 23 of 39 gonads in *lin-41(RNAi)*).

In the third assay, we examined whether the persistent GFP–γ-tubulin foci in proximal oocytes contain other PCM components

and centriolar proteins. In wild-type gonads, the PCM component SPD-5, which recruits γ-tubulin to centrosomes, localized to the vicinity of germ cell nuclei (GCN) from the distal gonad and disappeared at the diplotene stage, as observed for γ-tubulin distribution in the gonad (Figure 2B; wild-type, 31 of 31 gonads) (Mikeladze-Dvali *et al.*, 2012). Of importance, both SPD-5 and γ-tubulin foci at centrosomes were detectable in the LIN-41–depleted diakinetic oocytes (Figure 2B; *lin-41(RNAi)*, 73 of 73 gonads). By contrast, SPD-5 signal was not detectable in the ARF-1.2–depleted proximal oocytes even though these oocytes contained multiple clear γ-tubulin foci (Figure 2B; *arf-1.2(RNAi)*, 23 of 23 gonads). A similar result was obtained for staining of SAS-4, a centriolar protein, in the gonads of *lin-41(RNAi)* and *arf-1.2(RNAi)* animals (Figure 2C; 20 of 20 gonads for *lin-41(RNAi)* and 30 of 30 gonads for *arf-1.2(RNAi)*). We also found that centrosomal localization of SPD-5 and SAS-4 was detectable in *nmt-1(RNAi)* gonads only at the diplotene stage,
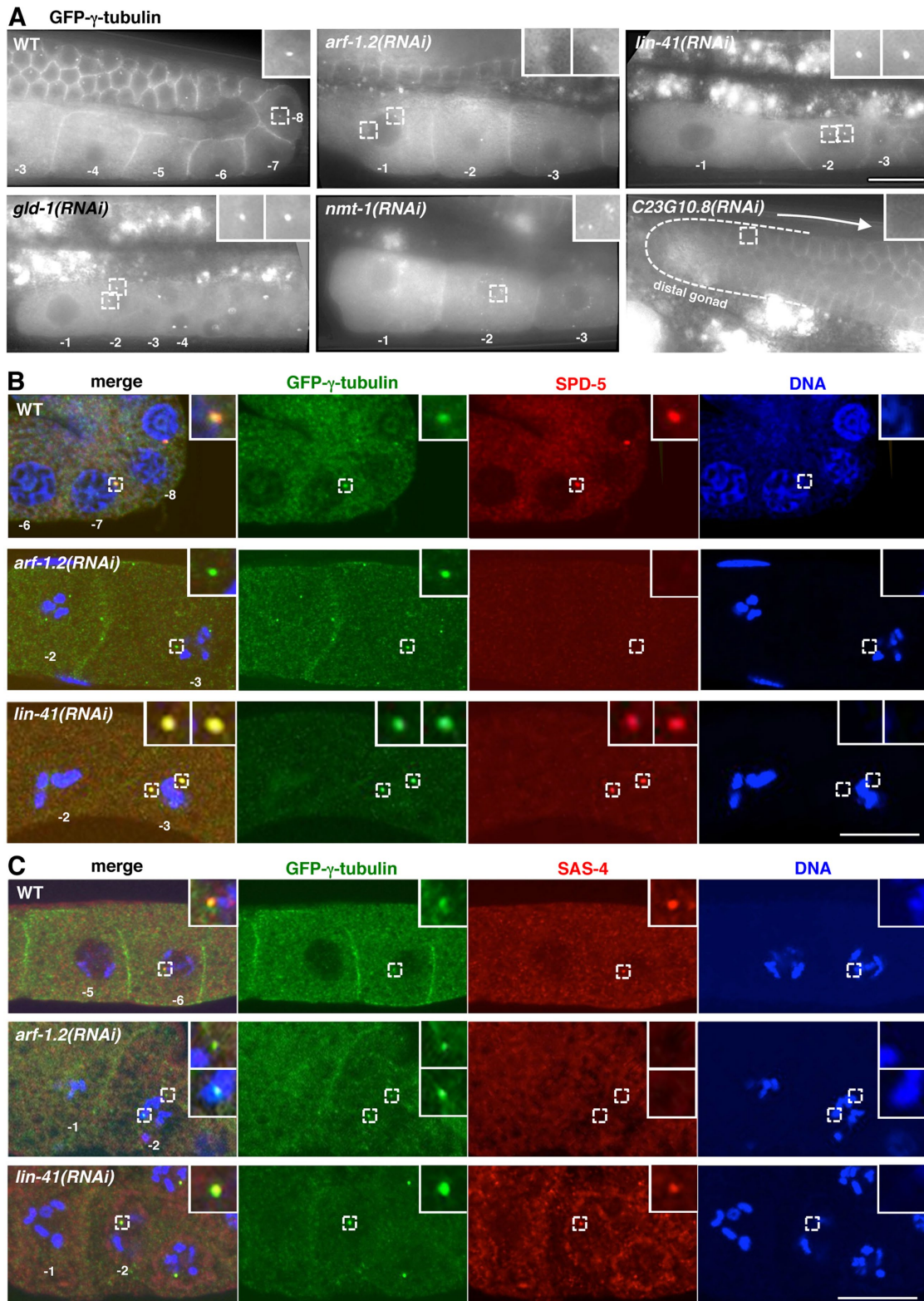
FIGURE 2: Defects in centrosome behavior in the hermaphrodite gonad upon RNAi-mediated inactivation of candidate genes. (A) Representative fluorescence images of gonads expressing GFP–γ-tubulin and treated with RNAi against the indicated genes. GFP–γ-tubulin foci detectable at the most proximal site of the gonads are shown in magnified insets. Inactivation of *C23G10.8* resulted in early elimination of GFP–γ-tubulin foci in the distal gonad. Insets are magnified threefold. Arrow shows the direction of germline development. (B, C) Immunostaining of hermaphrodite gonads expressing GFP–γ-tubulin in wild-type, *arf-1.2(RNAi)*, and *lin-41(RNAi)* with antibodies against SPD-5 (red in B), SAS-4 (red in C), and GFP (green). DNA is shown in blue. GFP–γ-tubulin foci detected at the most proximal site of the gonads are shown in magnified insets. Insets are magnified threefold. Numbers show positions of oocytes from the spermatheca. Scale bars, 10 μm.

although tiny ectopic GFP–γ-tubulin foci were found in the proximal oocytes, which was similar to the phenotype seen in *arf-1.2(RNAi)* gonads (Supplemental Figure S2, A and B). These results suggest that, whereas centrosome elimination was affected markedly by LIN-41 depletion, only γ-tubulin distribution was affected upon ARF-1.2 depletion independently of the occurrence of centrosome elimination.

Precocious γ-tubulin reduction affects gonad morphology but not PCM assembly and centriole integrity in female germ cells

Next we set out to characterize the detailed phenotype of the GFP–γ-tubulin elimination advance found in the first screening (Figure 1B). To examine whether early disappearance of GFP–γ-tubulin foci in the gonad reflects precocious elimination of PCM and centrioles, we immunostained RNAi-treated gonads using antibodies against SPD-5 and SAS-4 (Figure 3A and Supplemental Figure S2B). In *tbg-1(RNAi)* animals, in which the characteristic localization of γ-tubulin at centrosomes and plasma membranes in the gonad was diminished, the width of the rachis and position of the GCN in the gonad were affected, as previously reported (Figure 3B; Zhou *et al.*, 2009; Green *et al.*, 2011). Whereas the GCN were well aligned at the periphery in wild-type gonads, they were randomly located within the central rachis in *tbg-1(RNAi)* gonads. This defect probably reflects the lack of nuclear anchoring of the GCN with the microtubule filaments formed from the membrane-associated γ-tubulin complexes (Zhou *et al.*, 2009). By contrast, both the centrosomal SPD-5 and centriolar SAS-4 foci were normal in the vicinity of the GCN from the distal gonad to the diplotene stage (Figure 3A; 18 of 18 gonads; and unpublished data).

We found that depletion of the CCT complex was similar to that observed in *tbg-1(RNAi)* gonads in terms of the localization of SPD-5 and SAS-4 and gonad morphology; including the arrangement of the GCN and membranes (Figure 3B and unpublished data). It is therefore possible that the CCT complex regulates the integrity and distribution of γ-tubulin in the gonad, which is crucial for maintaining proper gonad morphology (Melki *et al.*, 1993; Lundin *et al.*, 2008; Saegusa *et al.*, 2014). In *C23G10.8(RNAi)* animals, the signal intensity of SPD-5 foci seemed not to be affected, and these foci colocalized with a weak GFP–γ-tubulin signal in the distal gonad (Figure 3A; 14 of 15 gonads). Although GFP–γ-tubulin was precociously depleted from the vicinity of crescent nuclei in the TZ (Figure 3A; 15 of 15 gonads), the staining of membrane GFP–γ-tubulin, centrosomal SPD-5, and centriolar SAS-4 and the overall gonad morphology were not significantly affected in *C23G10.8(RNAi)* animals (Figure 3, A and B, and Supplemental Figure S2B). These results suggest that C23G10.8 protein specifically regulates the maintenance of centrosomal γ-tubulin in oogenesis. From these findings, we conclude that precocious reduction of γ-tubulin does not affect the PCM or centriole stability during oogenesis and that membrane γ-tubulin is crucial for the maintenance of proper gonad morphology.

Depletion of LIN-41 leads to a delay in centrosome elimination and to centrosome separation

Although previous studies reported that centrosomes remain in the proximal region of the gonads of the *lin-41*-null mutant (Spike *et al.*, 2014a; Tocchini *et al.*, 2014), the GCN that retained centrosomes in the proximal gonad did not appear to be in diplotene or diakinesis. This was presumably because the GCN precociously entered M phase from the pachytene stage without passing through diplotene and diakinesis. In addition, in the most proximal gonad of the

lin-41-null mutant, the germ cells undergo somatic-like differentiation and form teratomas. Therefore, to identify a potential role of LIN-41 in centrosome elimination during diplotene in female meiosis, we used several RNAi conditions to analyze the detailed phenotype elicited by LIN-41 depletion. The penetrance seemed to depend on the duration of feeding *lin-41(RNAi)*. Whereas the oocyte morphology and meiotic chromosomal behavior were generally not affected in the proximal gonads treated with *lin-41(RNAi)* for 12 h, the oocytes tended to be smaller and formed teratomas upon longer treatment with *lin-41(RNAi)* (Supplemental Figure S3A; Spike *et al.*, 2014a; Tocchini *et al.*, 2014). We also observed RME-2–positive mature oocytes in the proximal gonads treated with *lin-41(RNAi)* for 12 h. By contrast, in the severe RNAi condition (e.g., for 24 h), RME-2 localization was no longer detected in the proximal gonads, as reported in previous studies (Spike *et al.*, 2014a; Tocchini *et al.*, 2014). Accordingly, to investigate the precise time of centrosome elimination in *lin-41(RNAi)* oocytes, we used an antibody to intermediate filament antigen (IFA), a centriole marker in *C. elegans*, and the mild RNAi condition (12 h) to examine the centrioles in the oocytes. Remarkably, centrioles were frequently detectable even in diakinetic oocytes in the LIN-41–depleted proximal gonads (Figure 4, A and B; 50, 40, and 10% at –4, –3, and –2 oocytes, respectively, in *lin-41(RNAi)*, compared with 2, 0, and 0% in wild type). However, we found no centrioles in the most proximal (–1) oocytes.

It was previously reported that disengaged centrioles exist adjacent to each other after meiotic entry and are simultaneously eliminated without separation at the diplotene stage (Mikeladze-Dvali *et al.*, 2012). However, intriguingly, centrosome separation occurred in LIN-41–depleted oocytes around late pachytene (Figure 4C; 88% in *lin-41(RNAi)* gonads [*n* = 33], compared with 0% in wild-type gonads [*n* = 28]). We then examined whether the anomalous centrosome behavior in *lin-41(RNAi)* gonads depends on the PCM. We treated *lin-41(RNAi)* on top of the *spd-5(or213)* mutant background, whose PCM assembly is defective. In this situation, the phenotype of centriole elimination delay was not significantly altered in the proximal oocytes (Figure 4, A and B; centrioles detected by 52, 22, and 7%, respectively, at –4, –3, and –2 oocytes in *spd-5(or213);lin-41(RNAi)* animals). We still detected diakinetic oocytes that harbored remaining centrioles (Figure 4A). By contrast, the ectopic centrosome separation induced upon LIN-41 depletion was partially suppressed by concomitant inactivation of *spd-5* (Figure 4C; 88% in *lin-41(RNAi)* gonads [*n* = 33], compared with 38% in *spd-5(or213);lin-41(RNAi)* gonads [*n* = 26]). Overall, these results suggest that LIN-41 regulates the time of centriole elimination in developing oocytes in a PCM-independent manner. On the other hand, the ectopic centrosome separation induced by LIN-41 depletion might be PCM dependent, at least in part.

Depletion of LIN-41 induces ectopic centrosome activation during oogenesis

Recent studies showed that, in the proximal gonad of *lin-41*-null mutants, ectopic centrosome activation occurs at the GCN that precociously proceeded in M phase or in the somatically differentiated state (Spike *et al.*, 2014a; Tocchini *et al.*, 2014). To test whether the milder depletion of LIN-41 also induces ectopic centrosome activation when meiotic progression of GCN appears not to be significantly affected, we monitored the MTOC activity of centrosomes in the gonads treated with mild *lin-41(RNAi)*. In the wild type, in which the centrosomes have already lost the MTOC activity around the TZ, signals from TAC-1, a PCM marker that should reflect the MTOC activity of centrosomes, were never observed in the loop region of the gonads (Figure 5, A and B; 42 of 42 gonads). By contrast, a
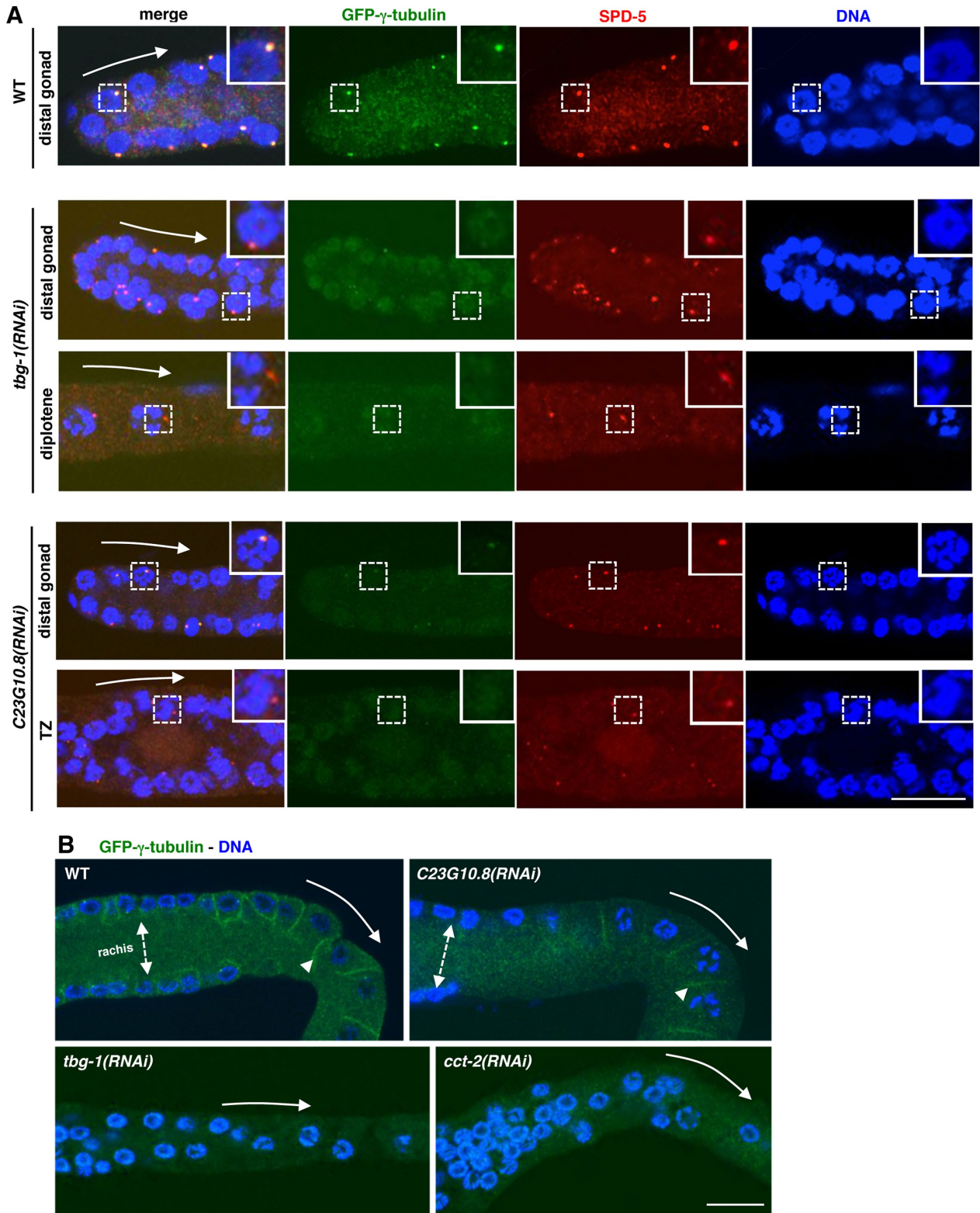
FIGURE 3: Precocious γ–tubulin reduction affects gonad morphology but not PCM assembly and centriole integrity in female germ cells. (A) Immunostaining of hermaphrodite gonads expressing GFP–γ-tubulin in wild-type, *tbg-1(RNAi)*, and *C23G10.8(RNAi)* with antibodies against GFP (green) and SPD-5 (red). DNA is shown in blue. Representative centrosomes and nuclei are indicated in magnified insets. Insets are magnified twofold. TZ, transition zone. (B) Immunostaining of the loop region of hermaphrodite gonads expressing GFP–γ-tubulin in wild-type, *tbg-1(RNAi)*, *C23G10.8(RNAi)*, and *cct-2(RNAi)* with antibodies against GFP (green). DNA is shown in blue. The dashed arrow shows the width of rachis at the pachytene stage. Note that the arrangement of GCN in the gonad was not affected in *C23G10.8(RNAi)* (n = 13) but was severely affected in *tbg-1(RNAi)* (9) and *cct-2(RNAi)* (26). Arrowheads indicate the membrane-bound GFP-γ-tubulin. Arrow shows the direction of germline development. Scale bars, 10 μm.
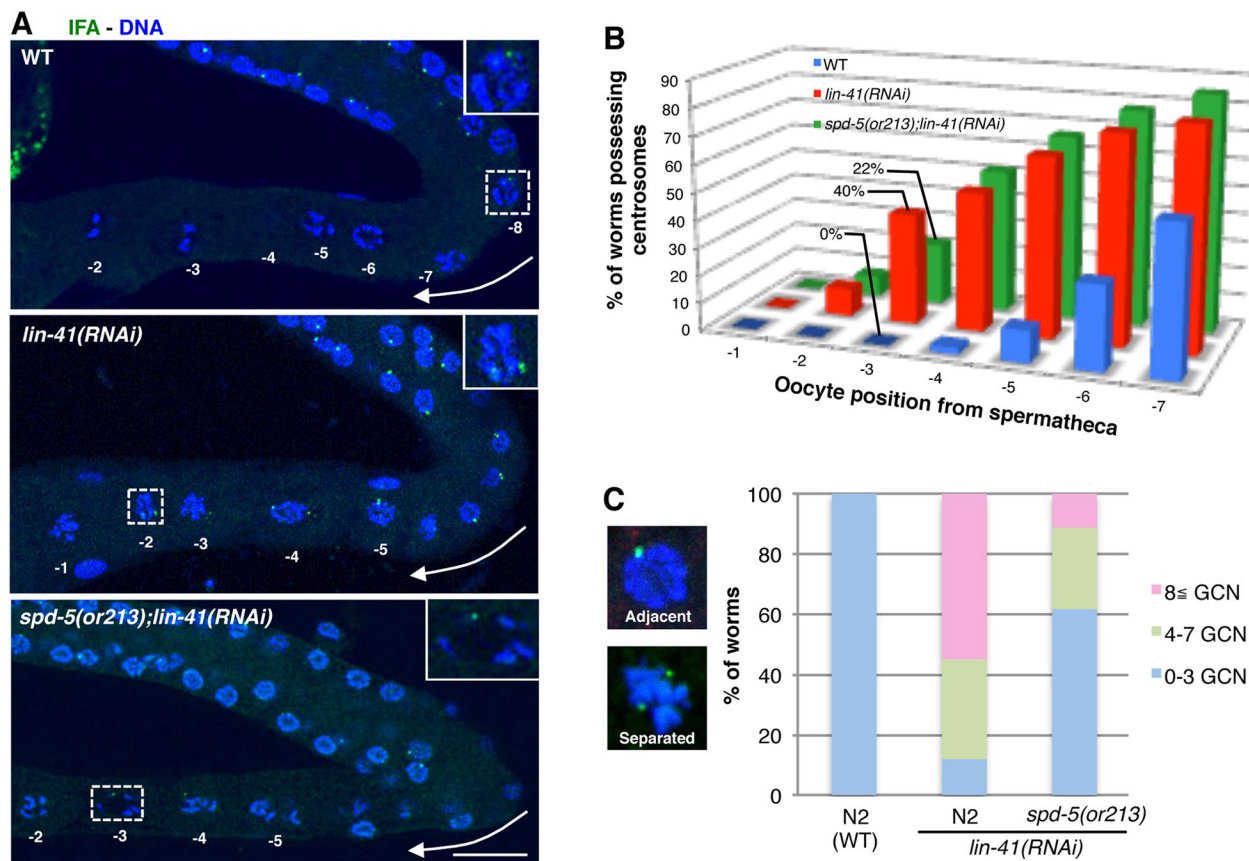
FIGURE 4: Depletion of LIN-41 leads to centrosome elimination delay and centrosome separation. (A) Immunostaining of wild-type, *lin-41(RNAi)*, and *spd-5(or213);lin-41(RNAi)* hermaphrodite gonads with centriolar marker IFA (green). DNA is shown in blue. N2 or *spd-5(or213)* temperature-sensitive mutant animals were treated with *lin-41(RNAi)* for 12 h at the restrictive temperature. Representative centriole signals are shown in magnified insets. Insets are magnified twofold. Arrow shows the direction of germline development. Numbers show positions of oocytes from the spermatheca. Scale bar, 10 μm. (B) Quantitation of the time of centrosome elimination in wild-type, *lin-41(RNAi)*, and *spd-5(or213);lin-41(RNAi)* oocytes, measured in the experiments illustrated in A. The number of worms possessing a centriolar IFA signal in the oocyte at the corresponding position from the spermatheca is indicated. Data shown are from three independent experiments: *n* = 43 for wild-type, 20 for *lin-41(RNAi)*, and 27 for *spd-5(or213);lin-41(RNAi)* hermaphrodites. (C) Quantitation of the frequency of centrosome separation in late pachytene of wild-type, *lin-41(RNAi)*, and *spd-5(or213);lin-41(RNAi)* gonads, measured in the experiments illustrated in A. Representative images showing adjacent and separated centrosome pairs. For each animal, the number of GCN with separated centrosomes was counted from late pachytene to proximal oocytes. Data shown are from three independent experiments: *n* = 28 for wild-type, 33 for *lin-41(RNAi)*, and 26 for *spd-5(or213);lin-41(RNAi)* hermaphrodites.

substantial number of activated centrosomes with ectopic TAC-1 signals were present around the loop region of the gonad under mild *lin-41(RNAi)* (Figure 5, A–C). Although the activated centrosomes were detectable just after late pachytene stage (Figure 5A), centrosomes in diakinetic oocytes seemed to be inactive in the proximal gonad.

The number of ectopic TAC-1 foci increased with increasing duration of RNAi treatment (Figure 5B). Under the severe RNAi condition, *lin-41(RNAi)* animals frequently exhibited small and disorganized oocytes with condensed nuclei and activated centrosomes in the proximal gonad, in addition to the GCN with activated centrosomes just after pachytene (*lin-41(24hr)* in Figure 5A). A similar phenotype was also found in the *lin-41* mutants *ma104* and *n2914*, as previously reported (Supplemental Figure S3B; Spike *et al.*, 2014a; Tocchini *et al.*, 2014). The MTOC activity of centrosomes at the loop or proximal region of the gonad was observed in *lin-41(ma104)* (30%, *n* = 20) and *lin-41(n2917)* (100%, *n* = 9) mutants (Supplemental Figure S3B). Because *lin-41(n2914)* is a null allele that leads to a

frameshift that is predicted to result in a premature stop codon, a stronger phenotype was detected. This contrasts with *ma104*, which does not behave as a null allele but instead as a reduction-of-function allele (Slack *et al.*, 2000). We also examined whether progression through the pachytene stage is needed to trigger these events in *lin-41(RNAi)* gonads. To arrest meiotic progression in the pachytene stage, we used an *mpk-1(ga111)* mutant in conjunction with *lin-41(RNAi)* treatment. In the *mpk-1(ga111)* background, over- all *lin-41(RNAi)* phenotype was not detected (Supplemental Figure S3C; 12 of 12 gonads), indicating that reduction of LIN-41 leads to ectopic activation of centrosomes and microtubule nucleation after the pachytene stage in oogenesis.

We also tested whether the heterochronic genes *let-7* and *lin-29* are implicated in the function of LIN-41 in oogenesis, because *lin-41* is known to act in the heterochronic pathway in somatic cells (Reinhart *et al.*, 2000; Slack *et al.*, 2000). As previously reported, the ectopic centrosome activation and other accompanying phenotypes were not rescued in the *let-7(mg279);lin-41(RNAi)* (24 of 24)
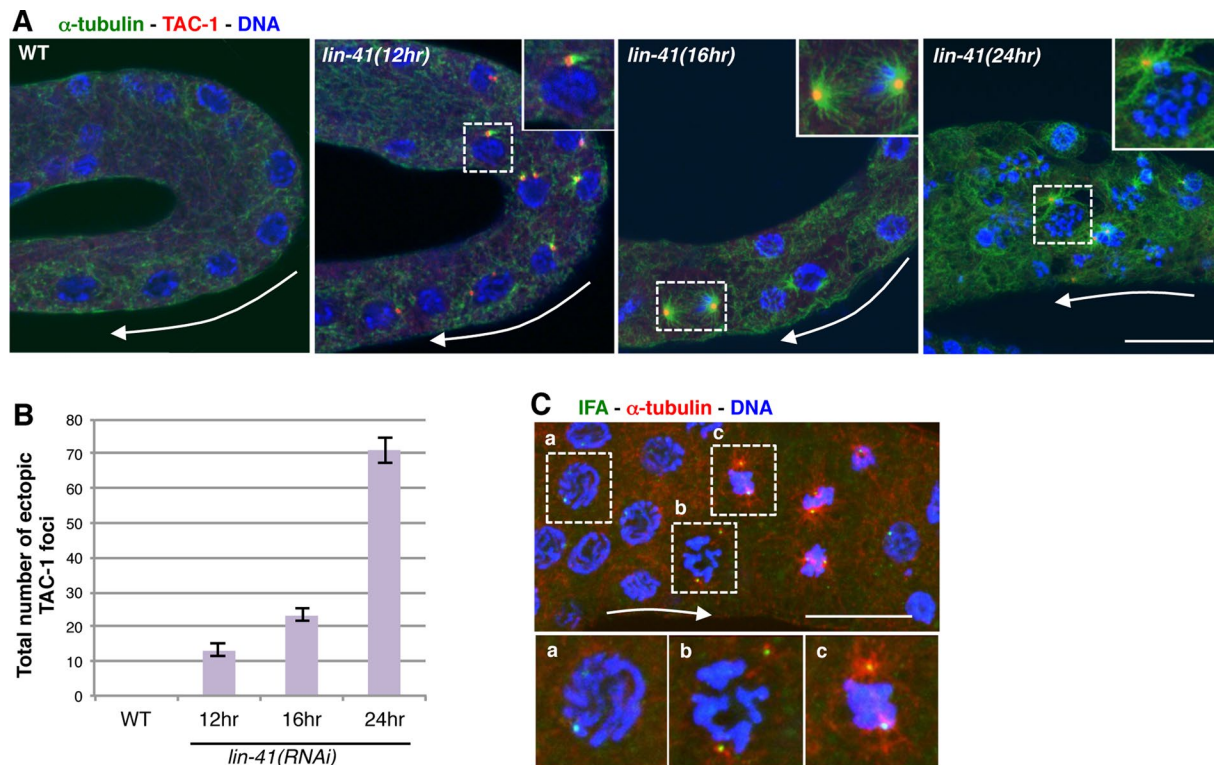
FIGURE 5: Depletion of LIN-41 induces ectopic centrosome activation. (A) Immunostaining of the loop region of wild-type and *lin-41(RNAi)* gonads with antibodies against α-tubulin (green) and PCM marker TAC-1 (red). DNA is shown in blue. Representative ectopic MTOCs are shown in magnified insets. Insets are magnified twofold. *lin-41(RNAi)* was performed for the indicated duration. (B) Quantitation of the average number of ectopic TAC-1 foci from pachytene to proximal oocytes in A. Values are mean ± SEM from three independent experiments: n = 28 for wild type, 14 for *lin-41(RNAi)* 12 h, 19 for *lin-41(RNAi)* 16 h, and 6 for *lin-41(RNAi)* 24 h. (C) The processes of ectopic centrosome activation in late pachytene of *lin-41(RNAi)* gonads. Immunostaining of the loop region of *lin-41(RNAi)* gonads with antibodies against IFA (green) and α-tubulin (red). DNA is shown in blue. (a) Pachytene nucleus with a centrosome pair; (b) initiation of microtubule nucleation at separated centrosomes; (c) highly condensed chromosomes and metaphase-like spindle formation with two activated centrosomes. Representative GCN with centrosomes are shown in magnified insets. Insets are magnified twofold. N2 hermaphrodites were treated with *lin-41(RNAi)* for 16 h. Arrow shows the direction of germline development. Scale bars, 10 μm.

or *lin-29(n482);lin-41(RNAi)* (23 of 23) gonads compared with *lin-41(RNAi)* gonads (30 of 31; Supplemental Figure S3D; Spike *et al.*, 2014a). Although we cannot exclude the possibility that the residual activity of LET-7 or LIN-29 in these mutants might suffice to exert the heterochronic pathway, these data strongly suggest that the heterochronic pathway is not implicated in centrosome behavior in oogenesis.

Ectopic spindles tried but failed to segregate the synapsed meiotic chromosomes after pachytene in LIN-41–depleted gonads

Next we set out to investigate the effect of ectopic centrosome activation on meiotic events in *lin-41(RNAi)* gonads. In wild-type gonads, nuclear envelope breakdown (NEBD) was never observed in the loop region because only the most proximal oocyte that receives the MSP signal for meiotic maturation induces NEBD (Harris *et al.*, 2006; Kim *et al.*, 2013). Although ectopic NEBD and condensed chromosomes were observed in the loop region of LIN-41–depleted gonads, presumably because of precocious M-phase entry (Supplemental Figure S4, A and B; Spike *et al.*, 2014a; Tocchini *et al.*, 2014), it is not clear how ectopic formation of spindles affects NEBD and chromosome condensation. We found that ectopic microtubule nucleation was detectable in late pachytene nuclei even

before NEBD (Figure 6A). After NEBD, formation of a bipolar spindle occurred, and this appeared to attempt to capture and segregate homologous chromosomes (Figure 6A).

To investigate further the abnormal chromosomal behavior during pachytene, we carefully monitored the synapsed homologous chromosome pairs, nuclear membrane, microtubule nucleation, and centrosomes in *lin-41(RNAi)* gonads. In wild-type gonads, HIM-3, which is a synaptonemal complex component, accumulated between sister chromatids, specifically during meiosis from the TZ to the proximal oocytes (Supplemental Figure S4C). In *lin-41(RNAi)* gonads, before NEBD, as TAC-1 foci began to accumulate on the surface of the nuclear membrane, HIM-3–positive chromosomes gathered into a cluster in the nucleus (Figure 6B). Of interest, during or after NEBD, all six chromosomes started to be pulled toward one of the two spindle poles (Figure 6B). At this stage, HIM-3 signals were retained on the chromosomes and gradually declined as bipolar spindle formation proceeded (Figure 6, C and D; HIM-3 absent in ~12% of GCN before NEBD, ~35% of GCN in metaphase-like, and ~54% of GCN after metaphase-like). After the metaphase-like event, although we could not detect properly segregated chromosomes, all chromosomes were in a blob and eventually captured by microtubules emanating from one of the two spindle poles (Figure 6, B, C, and E). Although the reason that all the synapsed
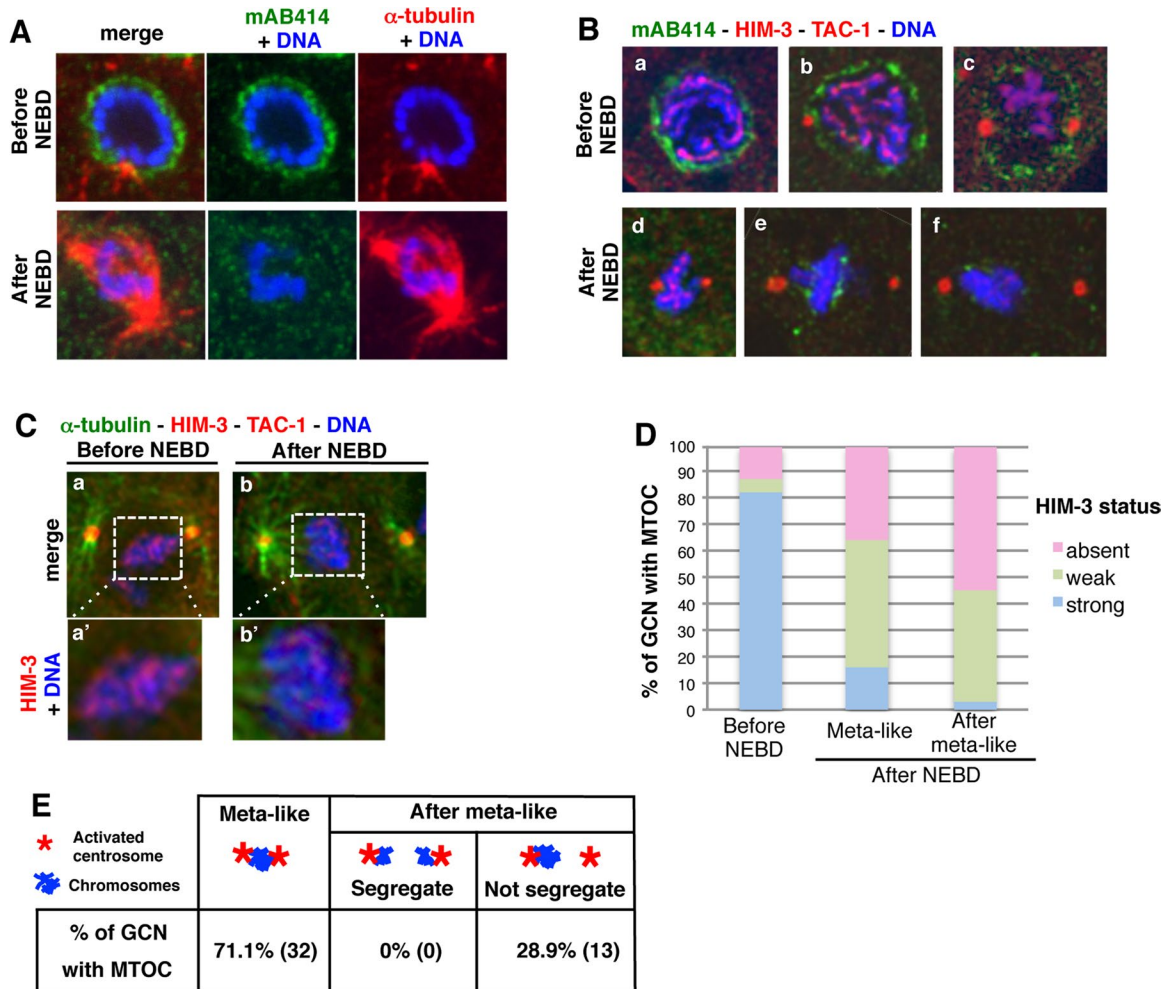
FIGURE 6: Depletion of LIN-41 leads to abnormal behavior of meiotic chromosomes during oogenesis. (A) Immunostaining of *lin-41(RNAi)* hermaphrodite gonads with antibodies for nuclear pore complex marker mAB414 (green) and α-tubulin (red). DNA is shown in blue. Top, a nucleus with an active centrosome before NEBD. Bottom, a bipolar spindle capturing condensed chromosomes after ectopic NEBD. N2 hermaphrodites were treated with *lin-41(RNAi)* for 16 h. (B) Immunostaining of *lin-41(RNAi)* hermaphrodite gonads with antibodies against mAB414 (green), meiotic chromosome marker HIM-3 (red), and TAC-1 (red). DNA is shown in blue. (a–c) Before NEBD: (a) early pachytene, (b) late pachytene nucleus with one TAC-1 signal, and (c) condensed nucleus with two TAC-1 signals. (d–f) After NEBD: (d) metaphase-like spindle and (e, f) a spindle after metaphase-like. (C) Immunostaining of *lin-41(RNAi)* gonads with antibodies against α-tubulin (green) TAC-1 (red), and HIM-3 (red). DNA is shown in blue. (a) GCN before NEBD and (b) GCN after NEBD with a spindle. HIM-3–positive chromosomes are captured and pulled toward the left pole. (a′, b′) Twofold magnified images of GCN. (D) Quantification of the frequency of GCN with the indicated HIM-3 status in the loop region of *lin-41(RNAi)* gonads, measured in the experiments illustrated in C. For each GCN with microtubule nucleation, HIM-3 levels were assessed and classified into three categories. Data shown are from three independent experiments: n = 39 for before NEBD, 31 for metaphase-like spindles after NEBD, and 33 for spindles after metaphase-like. (E) Quantification of the frequency of the indicated phenotypes on ectopic chromosome segregation in the gonads treated with *lin-41(RNAi)*. The experiments were performed as in C. Data shown are from three independent experiments, and the number of GCN with the indicated phenotypes is shown.

chromosome pairs were pulled together toward one of the two centrosomes is unclear, these results indicate that, in *lin-41(RNAi)* gonads, ectopically nucleating microtubules at centrosomes affect the behavior of meiotic chromosomes after the late pachytene stage. It is possible that the physical association of homologous chromosomes via the remaining synaptonemal complexes perturbs proper chromosome segregation.

In the severe *lin-41*(RNAi) condition or on the *lin-41*–mutant background, condensed chromosomes without HIM-3 signal were segregated equally by ectopic spindles in the proximal gonads, as previously reported (Spike *et al.*, 2014a). We assume that such GCN

were probably in a somatically differentiated state, because they were found mainly in teratoma-like small oocytes.

CDK-1/cyclin B regulates ectopic centrosome activation but not timely centrosome elimination and centrosome separation upon LIN-41 depletion

The CDK-1/cyclin B complex, which is the MPF, is required for both mitotic and meiotic spindle formation with or without centrosomes (McCarter *et al.*, 1999; Burrows *et al.*, 2006; Kim *et al.*, 2010). Because a recent study showed that the phenotype in the female germline of the *lin-41*–null mutant was rescued by inactivation of
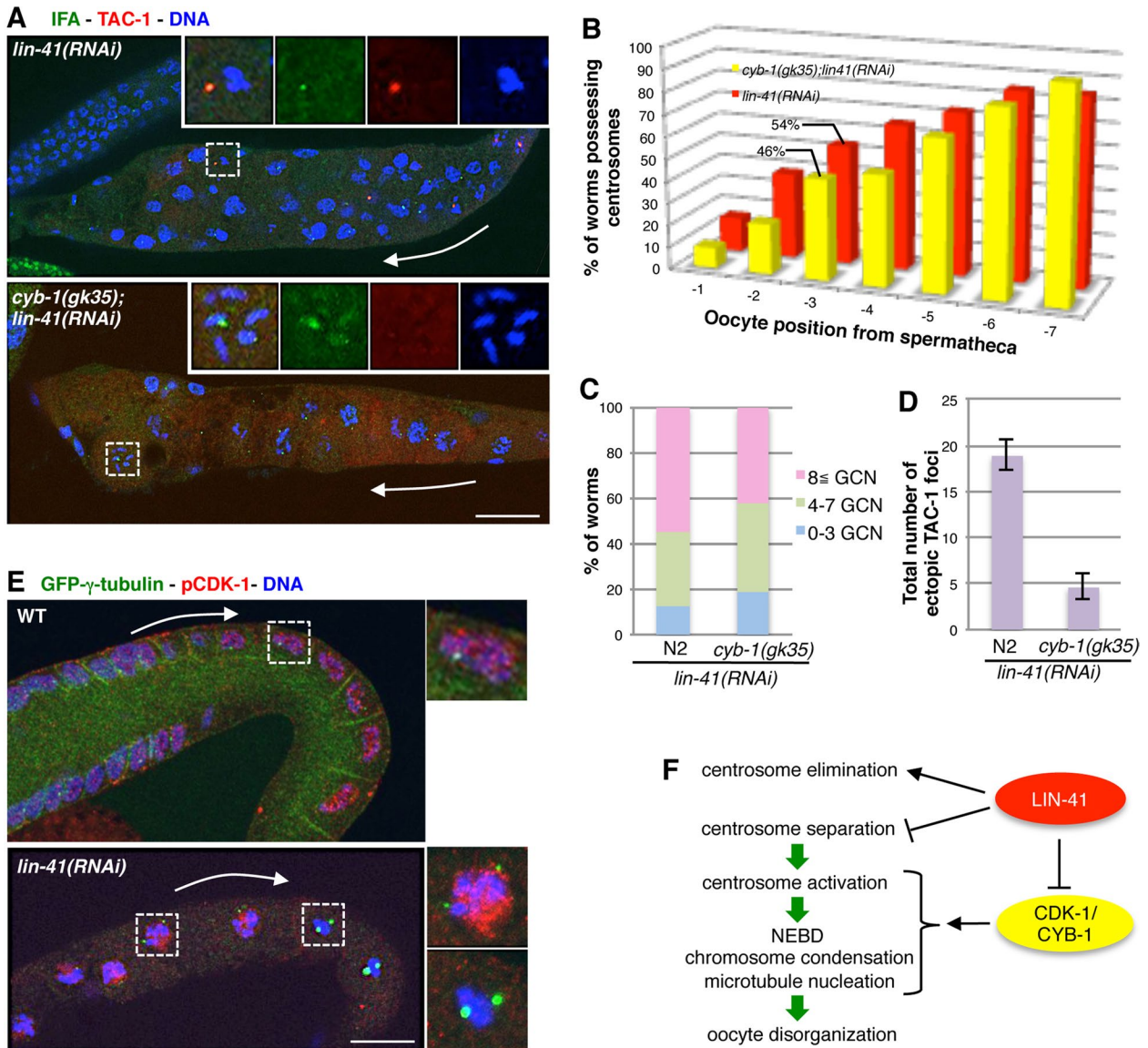
FIGURE 7: CDK-1/cyclin B pathway regulates ectopic centrosome activation but not timely centrosome elimination and centrosome separation upon LIN-41 depletion. (A) Immunostaining of *lin-41(RNAi)* and *cyb-1(gk35);lin-41(RNAi)* hermaphrodite gonads with antibodies against IFA (green) and TAC-1 (red). DNA is shown in blue. Representative GCN with IFA signal are shown in magnified insets. Insets are magnified threefold. N2 or *cyb-1(gk35)* hermaphrodites were treated with *lin-41(RNAi)* for 16 h. (B) Quantitation of the time of centrosome elimination in *lin-41(RNAi)* and *cyb-1(gk35);lin-41(RNAi)* oocytes, measured in the experiments illustrated in A. The number of worms possessing a centriolar IFA signal in the oocyte at the corresponding position from the spermatheca is indicated. Data shown are from three independent experiments: $n = 26$ for *lin-41(RNAi)* and 22 for *cyb-1(gk35);lin-41(RNAi)* hermaphrodites. (C) Quantitation of the frequency of centrosome separation in late pachytene of *lin-41(RNAi)* and *cyb-1(gk35);lin-41(RNAi)* gonads, measured in the experiments illustrated in A. For each animal, the number of GCN with separated centrosomes was counted from late pachytene to proximal oocytes. Data shown are from three independent experiments: $n = 33$ for *lin-41(RNAi)* and 35 for *cyb-1(gk35);lin-41(RNAi)* hermaphrodites. (D) Quantitation of the average number of ectopic TAC-1 foci from pachytene to proximal oocytes in A. Values are mean ± SEM from three independent experiments: $n = 33$ for *lin-41(RNAi)* and 35 for *cyb-1(gk35);lin-41(RNAi)*. (E) Immunostaining of LIN-41–depleted gonads expressing GFP–γ-tubulin with antibodies against inactive form of CDK-1 (pCDK-1) (red) and GFP (green). DNA is shown in blue. Representative GCN with GFP–γ-tubulin signal are shown in magnified insets. Insets are magnified twofold. N2 hermaphrodites were treated with *lin-41(RNAi)* for 16 h. (F) Model suggesting how the LIN-41 pathway regulates centrosome behavior and suppresses precocious M-phase events during oogenesis. Arrow shows the direction of germline development. Scale bars, 10 μm.

cdk-1 (Spike *et al.*, 2014a), we next focused on centrosome behavior upon LIN-41 depletion in the *cyb-1/cdk-1* mutant background. As previously reported, M phase–like events, including NEBD, chromosome condensation, and centrosome activation, were suppressed in the gonads of *cyb-1(gk35);lin-41(RNAi)* (Figure 7, A and D, and Supplemental Figure S5, A–D). As a consequence, the HIM-3 diminution seen in *lin-41(RNAi)* gonads was not observed in the gonads of *cyb-1(gk35);lin-41(RNAi)* (Figure 6B and Supplemental Figure S5B).

To examine whether LIN-41 affects CDK-1 activity during oogenesis, we stained LIN-41–depleted gonads with phospho–CDK-1 (pCDK-1) antibody, which specifically detects the inactive form of CDK-1 (Figure 7E and Supplemental Figure S5E; D'Angiolella et al., 2007; Kim et al., 2010). In wild-type gonads, pCDK-1 accumulated in the GCN from late pachytene to proximal oocytes (25 of 25). Although pCDK-1 initially accumulated in the GCN at late pachytene in LIN-41–depleted gonads, the signal disappeared around the loop region where condensed chromosomes were detected (Supplemental Figure S5E; 23 of 38 gonads). Of interest, centrosome separation was already recognizable in nuclei that contained pCDK-1 (Figure 7E; 14 of 21 gonads), suggesting that CDK-1 activation is dispensable for the centrosome separation found in lin-41(RNAi) gonads. We also found that pCDK-1 was absent from the nuclei that showed highly condensed chromosomes and microtubule asters (Figure 7E and Supplemental Figure S5F; 33 of 33 GCN).

Of importance, we found that the delay in centrosome elimination and centrosome separation were not rescued in cyb-1(gk35);lin-41(RNAi) animals (Figure 7, A–C; centrioles detected, 65, 54, and 39%, respectively, at −4, −3, and −2 lin-41(RNAi) oocytes vs. 50, 46, and 23% at −4, −3, and −2 cyb-1(gk35);lin-41(RNAi) oocytes; centriole separation, 88% in lin-41(RNAi) gonads vs. 81% in cyb-1(gk35);lin-41(RNAi) gonads). The remaining centrioles were found in diakinetic oocytes in the proximal region of cyb-1(gk35);lin-41(RNAi) gonads (Figure 7A). The same was also true when we tested lin-41(RNAi) in the cdk-1(ne2257) loss-of-function mutant background (Supplemental Figure S5C; 29 gonads). Taken together, these results suggest that whereas precocious M-phase events depend on CDK-1 activity, the delay in centrosome elimination and centrosome separation occurs independently of CDK-1 activity in lin-41(RNAi) gonads (Figure 7F).

DISCUSSION
We sought to identify critical genes that control in the behavior of centrosomes in oogenesis by using RNAi-mediated reduction of the maternal expression of essential genes in C. elegans. Although the RNAi screening failed to show retention of maternally contributed centrosomes to the zygotes as a phenotype, we found that inactivation of some essential genes resulted in a significant delay in centrosome elimination during C. elegans oogenesis. Given that, in almost all cases, centrosomes eventually disappeared in the most proximal (−1) oocyte, it might be that meiotic maturation in the −1 oocyte somehow involves a surveillance system for centrosome elimination. Alternatively, it is also possible that multiple factors redundantly promote centrosome elimination, which would make it difficult to completely block centrosome elimination solely by inactivation of a single gene. It has been reported that the XX karyotype of germ cells is critical to the timely removal of centrosomes during oogenesis (Mikeladze-Dvali et al., 2012). This raises the possibility that the transcription of genes on the X chromosomes in late pachytene and early diplotene may be implicated in centrosome elimination. It will be interesting to examine the influence of inactivation of a single or combination of X chromosome genes on centrosome elimination.

In most metazoans, γ-tubulin is critical for microtubule nucleation at centrosomes and regulation of microtubule organization. In C. elegans germ cells, γ-tubulin proteins localize not only to centrosomes but also at the plasma membrane in the syncytial gonad (Bobinnec et al., 2000; Zhou et al., 2009). Our screening identified several regulators of the unique subcellular localization of γ-tubulin in the germ cells of C. elegans. RNAi-mediated depletion of ARF-1.2 or NMT-1 led to the ectopic accumulation of γ-tubulin foci in the oocyte cytoplasm. By contrast, depletion of CCTs or C23G10.8

accelerated the elimination of γ-tubulin foci at centrosomes but not that of other PCM and centriole components. Although the exact function of C23G10.8 in the regulation of γ-tubulin in germ cells remains to be elucidated, it is possible that cytoplasmic chaperonin is required for the folding of γ-tubulin proteins, as reported in in vitro systems (Melki et al., 1993). Thus the behavior of γ-tubulin proteins at centrosomes seems to differ from that of other PCM and centriole components.

LIN-41 functions as a conserved heterochronic gene during the differentiation and development of somatic cells (Reinhart et al., 2000; Slack et al., 2000; Zou et al., 2013). Recent studies showed the novel function of LIN-41 in the female germline of C. elegans (Spike et al., 2014a; Tocchini et al., 2014). Using loss-of-function mutants of lin-41, Tocchini et al. (2014) showed that LIN-41 regulates the germ-to-soma transition and normally suppresses precocious somatic gene expression in developing oocytes. In line with this, LIN-41 is expressed substantially in the cytoplasm of female germ cells from late pachytene to proximal oocytes. It is also likely that the function of LIN-41 as an E3 ubiquitin ligase is dispensable for the regulation of gene expression in the gonad. Tocchini et al. (2014) reported that RNAi-mediated depletion of LIN-29, which is believed to be epistatic to lin-41 in the heterochronic pathway, did not suppress the defects in the female germline of the lin-41 mutant. Thus it is likely that LIN-41 functions through distinct targets and/or mechanisms in germ and somatic cells.

Spike et al. (2014a,b) showed that LIN-41 has an opposing function against OMA-1 to regulate the prophase-to-M-phase meiotic transition in female germ cells of C. elegans. Precocious meiotic M-phase entry through the CDK-1 pathway was observed in LIN-41–compromised developing oocytes. They claimed that the ectopic somatic gene expression detected in the lin-41 loss-of-function mutant might result from a defect in meiotic progression. Using cyb-1 loss-of-function mutant, we confirmed that the similar phenotypes of precocious M-phase entry in LIN-41–compromised oocytes depend on ectopic CDK-1/CYB-1 activation. In addition, we found direct evidence of CDK-1 activation in oocytes, using a pCDK-1 antibody that specifically detects inactive CDK-1.

Of importance, we found that the significant delay in centrosome elimination in lin-41(RNAi) gonads appears to be largely independent of the CDK-1/cyclin B pathway and PCM assembly. This suggests that LIN-41 somehow plays a role in promoting centrosome elimination in developing oocytes through unknown function(s). To identify the time of centrosome elimination in oocytes, we carefully optimized the mild lin-41(RNAi) condition to not affect meiosis progression and oocyte maturation. Spike et al. (2014a,b) suggested that centrosomes need to undergo the diplotene stage for their elimination, but in our mild lin-41(RNAi) condition, a significant delay in centrosome elimination was observed in mature diakinetic oocytes after passage through the diplotene stage. However, we cannot exclude the possibility that shortening the diplotene stage or defects in oocyte growth might have indirectly delayed centrosome elimination in lin-41(RNAi) germ cells. Based on these results, it is tempting to speculate that LIN-41 regulates, at least in part, the gene expression required for timely centrosome elimination around the diplotene stage in female germ cells. This may represent a conserved system for the process in most metazoans.

MATERIALS AND METHODS
Nematode strains
Wild-type (N2), spd-5(or213) (Tsai and Ahringer, 2007), lin-41(ma104) (Slack et al., 2000), lin-41(n2914) (Slack et al., 2000), let-7(mg279)

(Reinhart *et al.*, 2000), *lin-29(n482)* (Newman *et al.*, 2000), *cyb-1(gk35)* (CGC VC50), *cdk-1(ne2257)* (Shirayama *et al.*, 2006), *mpk-1(ga111)* (Lee et al., 2007), and transgenic animals expressing GFP–γ-tubulin (TBG-1-GFP; Hannak *et al.*, 2001) were maintained according to standard procedures (Brenner, 1974).

RNA interference and screening procedure
RNAi-mediated inactivation was done essentially as described (Delattre *et al.*, 2006), using feeding strains from the Ahringer library (Kamath *et al.*, 2003). We targeted available 513 genes out of 554 sterile genes known to be essential for proper embryo production and maintenance of gonad morphology (Green *et al.*, 2011). In the first screen, at least 10 L4 GFP–γ-tubulin animals were placed on each feeding RNAi plate at 25°C for 24 h. Then, using fluorescence microscopy, the time of disappearance of GFP–γ-tubulin foci as an indicator of centrosomes in the gonad was analyzed. Each gonad morphology in general was roughly described using reference from Green's phenotypic categories. As a lethality assessment, the percentage of embryos that fail to hatch was calculated from at least 50 embryos for each RNAi. The candidate genes that showed defects in GFP–γ-tubulin behavior in the gonad were subsequently assessed in the second screening (RME-2 staining for testing oocyte maturation) and third screening (SPD-5 and SAS-4 staining for testing PCM and centriole integrity). For the 4 candidate genes (Figure 1B), the same experiments were performed three times. We also confirmed the vectors encoding the candidate genes for feeding RNAi by DNA sequencing. For *lin-41(RNAi)*, inactivation was achieved by placing L4 larvae at 25°C for 12–24 h. For details of the screening, see Supplemental Table S1.

Antibodies
The following primary antibodies were used in this study: rabbit polyclonal antibodies against SAS-4 (1:1000; Santa Cruz Biotechnology, Dallas, TX), SPD-5 (1:2000; a gift from Bruce Bowerman, University of Oregon, Eugene, OR), RME-2 (1:200; a gift from Barth Grant, Rutgers University, Piscataway, NJ), CDK-1 phosphorylated-Tyr15 (1:100; Merck, Darmstadt, Germany), HIM-3 (1:500; Novus, Littleton, CO), TAC-1 (1:1000; Bellanger and Gonczy, 2003), α-tubulin (1:500; ab18251; Abcam, Cambridge, UK); and mouse monoclonal antibodies against mAB414 (1:1000; Abcam), IFA (1:50; American Type Culture Collection, Manassas, VA), GFP (1:50; a gift from Viestrurs Simanis, EPFL, Lausanne, Switzerland), and α-tubulin (1:3000, DM1α; Sigma-Aldrich, St. Louis, MO). We used the secondary antibodies Alexa Fluor 488 goat anti-mouse immunoglobulin G (IgG; H+L) and Alexa Fluor 568 goat anti-rabbit IgG (H+L), both at 1:500 (Thermo Fisher Scientific, Waltham, MA).

Indirect immunofluorescence
Hermaphrodite gonads were fixed and stained essentially as described (Leidel *et al.*, 2005). Briefly, gonads were dissected in 20 μM levamisole in phosphate-buffered saline (PBS) on polylysine-coated slides and then an equal amount of 4% paraformaldehyde was added for 2 min. Slides were transferred onto the frozen metal plate and then fixed in ice-cold methanol for 10 s. Slides were washed with PBS for 10 min and PBS/0.05% Tween 20 (PBST) for 10 min. Then the slides were incubated for blocking in 2% bovine serum albumin for 30 min before incubation with primary antibodies overnight at 4°C. The slides were washed with PBST for 10 min three times and incubated with secondary antibodies for 1 h at room temperature. The slides were washed with PBST for 10 min three times and counterstained with 1 μg/ml Hoechst

33258 (Sigma-Aldrich) to reveal DNA for 5 min. Immunofluorescence experiments were repeated at least three times unless otherwise specified.

Microscopy
For the microscopic analysis, worms were placed in a drop of M9 buffer containing 1 mM levamizole on 2% agar pad and covered with a coverslip (Kimura and Kimura, 2012). Fluorescence images were obtained on a Zeiss Axioplan 2 microscope (Carl Zeiss, Oberkochen, Germany) with a 100×/1.4 numerical aperture plan-Apochromat objective. Indirect immunofluorescence was imaged on a Leica TCS SP8 confocal microscope (Leica Microsystems, Wetzlar, Germany). Optical sections were acquired every 0.3 μm. Images were processed using ImageJ (National Institutes of Health, Bethesda, MD) and Photoshop (Adobe Systems, San Jose, CA), preserving relative image intensities within a series.

REFERENCES
Bellanger JM, Gönczy P (2003). TAC-1 and ZYG-9 form a complex that promotes microtubule assembly in C. elegans embryos. Curr Biol 13, 1488–1498.

Bobinnec Y, Fukuda M, Nishida E (2000). Identification and characterization of Caenorhabditis elegans gamma-tubulin in dividing cells and differentiated tissues. J Cell Sci 113, 3747–3759.

Bornens M (2012). The centrosome in cells and organisms. Science 335, 422–426.

Bornens M, Gönczy P (2014). Centrosomes back in the limelight. Philos Trans R Soc Lond B Biol Sci 369, 1650.

Brenner S (1974). Caenorhabditis elegans. Methods 77, 71–94.

Buck SH, Chiu D, Saito RM (2009). The cyclin-dependent kinase inhibitors, cki-1 and cki-2, act in overlapping but distinct pathways to control cell cycle quiescence during C. elegans development. Cell Cycle 8, 2613–2620.

Burrows AE, Sceurman BK, Kosinski ME, Richie CT, Sadler PL, Schumacher JM, Golden A (2006). The C. elegans Myt1 ortholog is required for the proper timing of oocyte maturation. Development 133, 697–709.

Dae YK, Roy R (2006). Cell cycle regulators control centrosome elimination during oogenesis in Caenorhabditis elegans. J Cell Biol 174, 751–757.

D'Angiolella V, Palazzo L, Santarpia C, Costanzo V, Grieco D (2007). Role for non-proteolytic control of M-phase promoting factor activity at M-phase exit. PLoS One 2, e248.

Delattre M, Canard C, Gönczy P (2006). Sequential protein recruitment in C. elegans centriole formation. Curr Biol 16, 1844–1849.

Delattre M, Gönczy P (2004). The arithmetic of centrosome biogenesis. J Cell Sci 117, 1619–1630.

Francis R, Barton MK, Kimble J, Schedl T (1995). gld-1, a tumor suppressor gene required for oocyte development in Caenorhabditis elegans. Genetics 139, 579–606.

Gönczy P (2012). Towards a molecular architecture of centriole assembly. Nat Rev Mol Cell Biol 13, 425–435.

Gönczy P, Echeverri C, Oegema K, Coulson A, Jones SJM, Copley RR, Duperon J, Oegema J, Brehm M, Cassin E, *et al.* (2000). Functional genomic analysis of cell division in C. elegans using RNAi of genes on chromosome III. Nature 408, 331–336.

Grant B, Hirsh D (1999). Receptor-mediated endocytosis in the Caenorhabditis elegans oocyte. Mol Biol Cell 10, 4311–4326.

Green RA, Kao HL, Audhya A, Arur S, Mayers JR, Fridolfsson HN, Schulman M, Schloissnig S, Niessen S, Laband K, *et al.* (2011). A high-resolution C. elegans essential gene network based on phenotypic profiling of a complex tissue. Cell 145, 470–482.

Hannak E, Kirkham M, Hyman AA, Oegema K (2001). Aurora-A kinase is required for centrosome maturation in Caenorhabditis elegans. J Cell Biol 155, 1109–1115.

Hansen D, Hubbard EJ, Schedl T (2004). Multi-pathway control of the proliferation versus meiotic development decision in the Caenorhabditis elegans germline. Dev Biol 268, 342–357.

Harris JE, Govindan JA, Yamamoto I, Schwartz J, Kaverina I, Greenstein D (2006). Major sperm protein signaling promotes oocyte microtubule reorganization prior to fertilization in Caenorhabditis elegans. Dev Biol 299, 105–121.

Hubbard EJ, Greenstein D (2000). The Caenorhabditis elegans gonad: a test tube for cell and developmental biology. Dev Dyn 218, 2–22.

Kamath RS, Fraser AG, Dong Y, Poulin G, Durbin R, Gotta M, Kanapin A, Bot NL, Moreno S, Sohrmann M, *et al.* (2003). Systematic functional analysis of the Caenorhabditis elegans genome using RNAi. Nature 421, 231–237.

Kemp CA, Kopish KR, Zipperlen P, Ahringer J, O'Connell KF (2004). Centrosome maturation and duplication in C. elegans require the coiled-coil protein SPD-2. Dev Cell 6, 511–523.

Kim J, Kawasaki I, Shim YH (2010). cdc-25.2, a C. elegans ortholog of cdc25, is required to promote oocyte maturation. J Cell Sci 123, 993–1000.

Kim S, Spike C, Greenstein D (2013). Control of oocyte growth and meiotic maturation in C. elegans. Adv Exp Med Biol 757, 277–320.

Kimura K, Kimura A (2012). Rab6 is required for the exocytosis of cortical granules and the recruitment of separase to the granules during the oocyte-to-embryo transition in Caenorhabditis elegans. J Cell Sci 125, 5897–905.

Lee MH, Ohmachi M, Arur S, Nayak S, Francis R, Church D, Lambie E, Schedl T (2007). Multiple functions and dynamic activation of MPK-1 extracellular signal-regulated kinase signaling in Caenorhabditis elegans germline development. Genetics 177, 2039–2062.

Leidel S, Delattre M, Cerutti L, Baumer K, Gönczy P (2005). SAS-6 defines a protein family required for centrosome duplication in C. elegans and in human cells. Nat Cell Biol 7, 115–125.

Lundin VF, Srayko M, Hyman AA, Leroux MR (2008). Efficient chaperone-mediated tubulin biogenesis is essential for cell division and cell migration in C. elegans. Dev Biol 313, 320–334.

Manandhar G, Schatten H, Sutovsky P (2005). Centrosome reduction during gametogenesis and its significance. Biol Reprod 72, 2–13.

McCarter J, Bartlett B, Dang T, Schedl T (1999). On the control of oocyte meiotic maturation and ovulation in Caenorhabditis elegans. Dev Biol 205, 111–128.

Melki R, Vainberg IE, Chow RL, Cowan NJ (1993). Chaperonin-mediated folding of vertebrate actin-related protein and gamma-tubulin. J Cell Biol 122, 1301–1310.

Mikeladze-Dvali T, von Tobel L, Strnad P, Knott G, Leonhardt H, Schermelleh L, Gonczy P (2012). Analysis of centriole elimination during C. elegans oogenesis. Development 139, 1670–1679.

Newman AP, Inoue T, Wang M, Sternberg PW (2000). The Caenorhabditis elegans heterochronic gene lin-29 coordinates the vulval-uterine-epidermal connections. Curr Biol 10, 1479–1488.

Nigg EA, Stearns T (2011). The centrosome cycle: centriole biogenesis, duplication and inherent asymmetries. Nat Cell Biol 13, 1154–1160.

Reinhart BJ, Slack FJ, Basson M, Pasquinelli AE, Bettinger JC, Rougvie AE, Horvitz HR, Ruvkun G (2000). The 21-nucleotide let-7 RNA regulates developmental timing in Caenorhabditis elegans. Nature 403, 901–906.

Saegusa K, Sato M, Sato K, Nakajima-Shimada J, Harada A, Sato K (2014). Caenorhabditis elegans chaperonin CCT/TRiC is required for actin and tubulin biogenesis and microvillus formation in intestinal epithelial cells. Mol Biol Cell 25, 3095–3104.

Sathananthan AH, Ratnam SS, Ng SC, Tarín JJ, Gianaroli L, Trounson A (1996). The sperm centriole: its inheritance, replication and perpetuation in early human embryos. Hum Reprod 11, 345–356.

Schatten H, Sun QY (2009). The role of centrosomes in mammalian fertilization and its significance for ICSI. Mol Hum Reprod 15, 531–538.

Shirayama M, Soto MC, Ishidate T, Kim S, Nakamura K, Bei Y, Van Den Heuvel S, Mello CC (2006). The conserved kinases CDK-1, GSK-3, KIN-19, and MBK-2 promote OMA-1 destruction to regulate the oocyte-to-embryo transition in C. elegans. Curr Biol 16, 47–55.

Slack FJ, Basson M, Liu Z, Ambros V, Horvitz HR, Ruvkun G (2000). The lin-41 RBCC gene acts in the C. elegans heterochronic pathway between the let-7 regulatory RNA and the LIN-29 transcription factor. Mol Cell 5, 659–669.

Sönnichsen B, Koski LB, Walsh A, Marschall P, Neumann B, Brehm M, Alleaume AM, Artelt J, Bettencourt P, Cassin E, *et al.* (2005). Full-genome RNAi profiling of early embryogenesis in Caenorhabditis elegans. Nature 434, 462–469.

Spike CA, Coetzee D, Eichten C, Wang X, Hansen D, Greenstein D (2014a). The TRIM-NHL protein LIN-41 and the OMA RNA-binding proteins antagonistically control the prophase-to-metaphase transition and growth of Caenorhabditis elegans 0ocytes. Genetics 198, 1535–1558.

Spike CA, Coetzee D, Nishi Y, Guven-Ozkan T, Oldenbroek M, Yamamoto I, Lin R, Greenstein D (2014b). Translational control of the oogenic program by components of OMA ribonucleoprotein particles in Caenorhabditis elegans. Genetics 198, 1513–1533.

Tocchini C, Keusch JJ, Miller SB, Finger S, Gut H, Stadler MB, Ciosk R (2014). The TRIM-NHL protein LIN-41 controls the onset of developmental plasticity in Caenorhabditis elegans. PLoS Genet 10, e1004533.

Tsai MC, Ahringer J (2007). Microtubules are involved in anterior-posterior axis formation in C. elegans embryos. J Cell Biol 179, 397–402.

Zetka MC, Kawasaki I, Strome S, Muller F (1999). Synapsis and chiasma formation in Caenorhabditis elegans require HIM-3, a meiotic chromosome core component that functions in chromosome segregation. Genes Dev 13, 2258–2270.

Zhou K, Rolls MM, Hall DH, Malone CJ, Hanna-Rose W (2009). A ZYG-12-dynein interaction at the nuclear envelope defines cytoskeletal architecture in the C. elegans gonad. J Cell Biol 186, 229–241.

Zou Y, Chiu H, Zinovyeva A, Ambros V, Chuang CF, Chang C (2013). Developmental decline in neuronal regeneration by the progressive change of two intrinsic timers. Science 340, 372–376.